EURASIP Journal on Applied Signal Processing 2004:2, 236–252

New Complexity Scalable MPEG Encoding Techniques for Mobile Applications

Stephan Mietens
Philips Research Laboratories, Prof. Holstlaan 4, NL-5656 AA Eindhoven, The Netherlands
Email: stephan.mielens@philips.com

Peter H. N. de With
LogicaCMG Eindhoven, Eindhoven University of Technology, P.O. Box 7089, Luchthavenweg 57, NL-5600 MB Eindhoven, The Netherlands
Email: p.h.n.de.with@tue.nl

Christian Hentschel
Cottbus University of Technology, Universitätsplatz 3-4, D-03044 Cottbus, Germany
Email: christian.hentschel@tu-cottbus.de

Received 10 December 2002; Revised 7 July 2003

Complexity scalability offers the advantage of one-time design of video applications for a large product family, including mobile devices, without the need of redesigning the applications on the algorithmic level to meet the requirements of the different products. In this paper, we present complexity scalable MPEG encoding having core modules with modifications for scalability. The interdependencies of the scalable modules and the system performance are evaluated. Experimental results show scalability giving a smooth change in complexity and corresponding video quality. Scalability is basically achieved by varying the number of computed DCT coefficients and the number of evaluated motion vectors, but other modules are designed such they scale with the previous parameters. In the experiments using the "Stefan" sequence, the elapsed execution time of the scalable encoder, reflecting the computational complexity, can be gradually reduced to roughly 50% of its original execution time. The video quality scales between 20 dB and 48 dB PSNR with unity quantizer setting, and between 21.5 dB and 38.5 dB PSNR for different sequences targeting 1500 kbps. The implemented encoder and the scalability techniques can be successfully applied in mobile systems based on MPEG video compression.

Keywords and phrases: MPEG encoding, scalable algorithms, resource scalability.

1. INTRODUCTION

Nowadays, digital video applications based on MPEG video compression (e.g., Internet-based video conferencing) are popular and can be found in a plurality of consumer products. While in the past, mainly TV and PC systems were used, having sufficient computing resources available to execute the video applications, video is increasingly integrated into devices such as portable TV and mobile consumer terminals (see Figure 1).

Video applications that run on these products are heavily constrained in many aspects due to their limited resources as compared to high-end computer systems or high-end consumer devices. For example, real-time execution has to be assured while having limited computing power and memory for intermediate results. Different video resolutions have to be handled due to the variable displaying of video frame sizes. The available memory access or transmission bandwidth is limited as the operating time is shorter for computation-intensive applications. Finally the product success on the market highly depends on the product cost. Due to these restrictions, video applications are mainly redesigned for each product, resulting in higher production cost and longer time-to-market.

In this paper, it is our objective to design a scalable MPEG encoding system, featuring scalable video quality and a corresponding scalable resource usage [1]. Such a system enables advanced video encoding applications on a plurality of low-cost or mobile consumer terminals, having limited resources (available memory, computing power, stand-by time, etc.) as compared to high-end computer systems or high-end consumer devices. Note that the advantage of scalable systems is that they are designed once for a whole product family instead of a single product, thus they have a faster

FIGURE 1: Multimedia applications shown on different devices sharing the available resources.

time-to-market. State-of-the-art MPEG algorithms do not provide scalability, thereby hampering, for example, low-cost solutions for portable devices and varying coding applications in multitasking environments.

This paper is organized as follows. Section 2 gives a brief overview of the conventional MPEG encoder architecture. Section 3 gives an overview of the potential scalability of computational complexity in MPEG core functions. Section 4 presents a scalable discrete cosine transformation (DCT) and motion estimation (ME), which are the core functions of MPEG coding systems. Part of this work was presented earlier. A special section between DCT and ME is devoted to content-adaptive processing, which is of benefit for both core functions. The enhancements on the system level are presented in Section 5. The integration of several individual scalable functions into a full scalable coder has given a new framework for experiments. Section 6 concludes the paper.

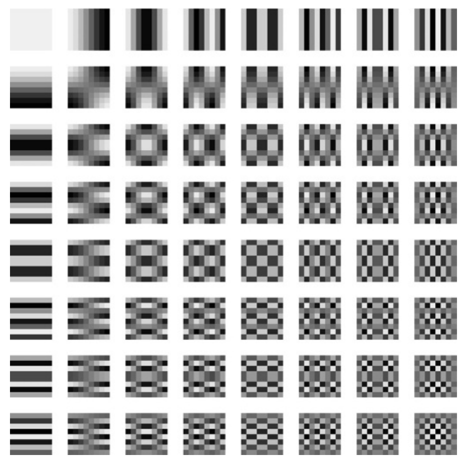

FIGURE 2: DCT block of basis patterns.

2. CONVENTIONAL MPEG ARCHITECTURE

The MPEG coding standard is used to compress a video sequence by exploiting the spatial and temporal correlations of the sequence as briefly described below.

Spatial correlation is found when looking into individual video frames (pictures) and considering areas of similar data structures (color, texture). The DCT is used to decorrelate spatial information by converting picture blocks to the transform domain. The result of the DCT is a block of transform coefficients, which are related to the frequencies contained in the input picture block. The patterns shown in Figure 2 are the representation of the frequencies, and each picture block is a linear combination of these basis patterns. Since high frequencies (at the bottom right of the figure) commonly have lower amplitudes than other frequencies and are less perceptible in pictures, they can be removed by quantizing the DCT coefficients.

Temporal correlation is found between successive frames of a video sequence when considering that the objects and background are on similar positions. For data compression purpose, the correlation is removed by predicting the contents and coding the frame differences instead of complete frames, thereby saving bandwidth and/or storage space. Motion in video sequences introduced by camera movements or moving objects result in high spatial frequencies occurring in the frame difference signal. A high compression rate is achieved by predicting picture contents using ME and motion compensation (MC) techniques.

For each frame, the above-mentioned correlations are exploited differently. Three different types of frames are defined in the MPEG coding standard, namely, I-, P-, and B-frames. I-frames are coded as completely independent frames, thus only spatial correlations are exploited. For P- and B-frames, temporal correlations are exploited, where P-frames use one temporal reference, namely, the past reference frame. B-frames use both the past and the upcoming reference frames, where I-frames and P-frames serve as reference frames. After MC, the frame difference signals are coded by DCT coding.

A conventional MPEG architecture is depicted in Figure 3. Since B-frames refer to future reference frames, they cannot be encoder/decoder before this reference frame is received by the coder (encoder or decoder). Therefore, the video frames are processed in a reordered way, for example, "IPBB" (transmit order) instead of "IBBP" (display order).

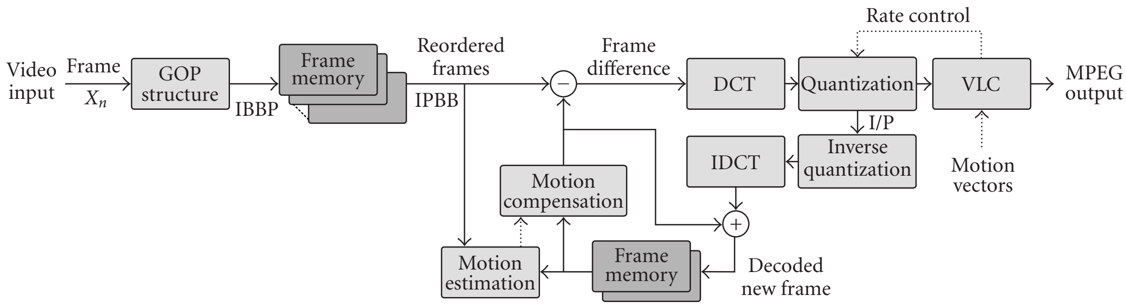

FIGURE 3: Basic architecture of an MPEG encoder.

Note that for the ME process, reference frames that are used are reduced in quality due to the quantization step. This limits the accuracy of the ME. We will exploit this property in the scalable ME.

3. SCALABILITY OVERVIEW OF MPEG FUNCTIONS

Our first step towards scalable MPEG encoding is to redesign the individual MPEG core functions (modules) and make them scalable themselves. In this paper, we concentrate mainly on scalability techniques on the algorithmic level, because these techniques can be applied to various sorts of hardware architectures. After the selection of an architecture, further optimizations on the core functions can be made. An example to exploit features of a reduced instruction set computer (RISC) processor for obtaining an efficient implementation of an MPEG coder is given in [2].

In the following, the scalability potentials of the modules shown in Figure 3 are described. Further enhancements that can be made by exploiting the modules interconnections are described in Section 5. Note that we concentrate on the encoder and do not consider pre- or postprocessing steps of the video signal, because such steps can be performed independently from the encoding process. For this reason, the input video sequence is modified neither in resolution nor in frame rate for achieving reduced complexity.

GOP structure

This module defines the types of the input frames to form group of pictures (GOP) structures. The structure can be either *fixed* (all GOPs have the same structure) or *dynamic* (content-dependent definition of frame types). The computational complexity required to define fixed GOP structures is negligible. Defining a dynamic GOP structure has a higher computational complexity, for example for analyzing frame contents. The analysis is used for example to detect scene changes. The rate distortion ratio can be optimized if a GOP starts with the frame following the scene change.

Both the fixed and the dynamic definitions of the GOP structure can control the computational complexity of the coding process and the bit rate of the coded MPEG stream with the ratio of I-, P-, and B-frames in the stream. In general, I-frames require less computation than P- or B-frames, because no ME and MC is involved in the processing of I-frames. The ME, which requires significant computational effort, is performed for each temporal reference that is used. For this reason, P-frames (having one temporal reference) are normally half as complex in terms of computations as B-frames (having two temporal references). It can be considered further that no inverse DCT and quantization is required for B-frames. For the bit rate, the relation is the other way around since each temporal reference generally reduces the amount of information (frame contents or changes) that has to be coded.

The chosen GOP structure has influence on the memory consumption of the encoder as well, because frames must be kept in memory until a reference frame (I- or P-frame) is processed. Besides defining I-, P-, and B-frames, input frames can be skipped and thus are not further processed while saving memory, computations, and bit rates.

The named options are not further worked out, because they can be easily applied on every MPEG encoder without the need to change the encoder modules themselves. A dynamic GOP structure would require additional functionality through, for example, scene change detection. The experiments that are made for this paper are based on a fixed GOP structure.

Discrete cosine transformation

The DCT transforms image blocks to the transform domain to obtain a powerful compression. In conjunction with the inverse DCT (IDCT), a perfect reconstruction of the image blocks is achieved while spending fewer bits for coding the blocks than not using the transformation. The accuracy of the DCT computation can be lowered by reducing the number of bits that is used for intermediate results. In principle, reduced accuracy can scale up the computation speed because several operations can be executed in parallel (e.g., two 8-bit operations instead of one 16-bit operation). Furthermore, the silicon area needed in hardware design is scaled down with reduced accuracy due to simpler hardware components (e.g., an 8-bit adder instead of a 16-bit adder). These two possibilities are not further worked out because they are not algorithm-specific optimizations and therefore are suitable for only a few hardware architectures.

An algorithm-specific optimization that can be applied on any hardware architecture is to scale down the number of DCT coefficients that are computed. A new technique, considering the baseline DCT algorithm and a corresponding architecture for finding a specific computation order of the coefficients, is described in Section 4.1. The computation order maximizes the number of computed coefficients for a given limited amount of computation resources.

Another approach for scalable DCT computation predicts at several stages during the computation whether a group of DCT coefficients are zero after quantization and their computation can be stopped or not [3].

Inverse discrete cosine transformation

The IDCT transforms the DCT coefficients back to the spatial domain in order to reconstruct the reference frames for the (ME) and (MC) process. The previous discussion on scalability options for the DCT also applies to the IDCT. However, it should be noted that a scaled IDCT should have the same result as a perfect IDCT in order to be compatible with the MPEG standard. Otherwise, the decoder (at the receiver side) should ensure that it uses the same scaled IDCT as in the encoder in order to avoid error drift in the decoded video sequence.

Previous work on scalability of the IDCT at the receiver side exists [4, 5], where a simple subset of the received DCT coefficients is decoded. This has not been elaborated because in this paper, we concentrate on the encoder side.

Quantization

The quantization reduces the accuracy of the DCT coefficients and is therefore able to remove or weight frequencies of lower importance for achieving a higher compression ratio. Compared to the DCT where data dependencies during the computation of 64 coefficients are exploited, the quantization processes single coefficients where intermediate results cannot be reused for the computation of other coefficients. Nevertheless, computing the quantization involves rounding that can be simplified or left out for scaling up the processing speed. This possibility has not been worked out further.

Instead, we exploit scalability for the quantization based on the scaled DCT by preselecting coefficients for the computation such that coefficients that are not computed by the DCT are not further processed.

Inverse quantization

The inverse quantization restores the quantized coefficient values to the regular amplitude range prior to computing the IDCT. Like the IDCT, the inverse quantization requires sufficient accuracy to be compatible with the MPEG standard. Otherwise, the decoder at the receiver should ensure that it avoids error drift.

Motion estimation

The ME computes motion vector (MV) fields to indicate block displacements in a video sequence. A picture block (macroblock) is then coded with reference to a block in a previously decoded frame (the prediction) and the difference to this prediction. The ME contains several scalability options. In principle, any good state-of-the-art fast ME algorithm offers an important step in creating a scaled algorithm. Compared to full search, the computing complexity is much lower (significantly less MV candidates are evaluated) while accepting some loss in the frame prediction quality. Taking the fast ME algorithms as references, a further increase of the processing speed is obtained by simplifying the applied set of motion vectors (MVs).

Besides reducing the number of vector candidates, the displacement error measurement (usually the sum of absolute pixel differences (SAD)) can be simplified (thus increase computation speed) by reducing the number of pixel values (e.g., via subsampling) that are used to compute the SAD. Furthermore, the accuracy of the SAD computation can be reduced to be able to execute more than one operation in parallel. As described for the DCT, this technique is suitable for a few hardware architectures only.

Up to this point, we have assumed that ME is performed for each macroblock. However, the number of processed macroblocks can be reduced also, similar to the pixel count for the SAD computation. MVs for omitted macroblocks are then approximated from neighboring macroblocks. This technique can be used for concentrating the computing effort on areas in a frame, where the block contents lead to a better estimation of the motion when spending more computing power [6].

A new technique to perform the ME in three stages by exploiting the opportunities of high-quality frame-by-frame ME is presented in Section 4.3. In this technique, we used several of the above-mentioned options and we deviate from the conventional MPEG processing order.

Motion compensation

The MC uses the MV fields from the ME and generates the frame prediction. The difference between this prediction and the original input frame is then forwarded to the DCT. Like the IDCT and the inverse quantization, the MC requires sufficient accuracy for satisfying the MPEG standard. Otherwise, the decoder (at the receiver) should ensure using the same scaled MC as in the encoder to avoid error drift.

Variable-length coding (VLC)

The VLC generates the coded video stream as defined in the MPEG standard. Optimization of the output can be made here, like ensuring a predefined bit rate. The computational effort is scalable with the number of nonzero coefficients that remain after quantization.

4. SCALABLE FUNCTIONS FOR MPEG ENCODING

Computationally expensive corner stones of an MPEG encoder are the DCT and the ME. Both are addressed in the scalable form in Section 4.1 on the scalable DCT [7] and in Section 4.3 on the scalable ME [8], respectively. Additionally, Section 4.2 presents a scalable block classification algorithm, which is designed to support and integrate the scalable DCT and ME on the system level (see Section 5).

4.1. Discrete Cosine Transformation

4.1.1. Basics

The DCT transforms the luminance and chrominance values of small square blocks of an image to the transform domain. Afterwards, all coefficients are quantized and coded. For a given $N \times N$ image block represented as a two-dimensional (2D) data matrix $\{X[i, j]\}$, where $i, j = 0, 1, \ldots, N-1$, the 2D DCT matrix of the coefficients $\{Y[m, n]\}$ with $m, n = 0, 1, \ldots, N-1$ is computed by

$$\begin{aligned} Y[m,n] &= \frac{4}{N^2} * u(m) * u(n) \\ &\quad * \sum_{i=0}^{N-1} \sum_{j=0}^{N-1} X[i,j] * \cos\frac{(2i+1)m * \pi}{2N} \\ &\quad * \cos\frac{(2j+1)n * \pi}{2N}, \end{aligned} \tag{1}$$

where $u(i) = 1/\sqrt{2}$ if $i = 0$ and $u(i) = 1$ elsewhere. Equation (1) can be simplified by ignoring the constant factors for convenience and defining a square cosine matrix K by

$$K_N[p,q] = \cos\frac{(2p+1)q * \pi}{2N} \tag{2}$$

so that (1) can be rewritten as

$$Y = K_N * X * K_N^\top. \tag{3}$$

Equation (3) shows that the 2D DCT as specified by (1) is based on two orthogonal 1D DCTs, where $K_N * X$ transforms the columns of the image block X, and $X * K_N^\top$ transforms the rows. Since the computation of two 1D DCTs is less expensive than one 2D DCT, state-of-the-art DCT algorithms normally refer to (3) and concentrate on optimizing a 1D DCT.

4.1.2. Scalability

Our proposed scalable DCT is a novel technique for finding a specific computation order of the DCT coefficients. The results depend on the applied (fast) DCT algorithm. In our approach, the DCT algorithm is modified by eliminating several computations and thus coefficients, thereby enabling complexity scalability for the used algorithm. Consequently, the output of the algorithm will have less quality, but the processing effort of the algorithm is reduced, leading to a higher computing speed. The key issue is to identify the computation steps that can be omitted to maximize the number of coefficients for the best possible video quality.

Since fast DCT algorithms process video data in different ways, the algorithm used for a certain scalable application should be analyzed closely as follows. Prior to each computation step, a list of remaining DCT coefficients is sorted

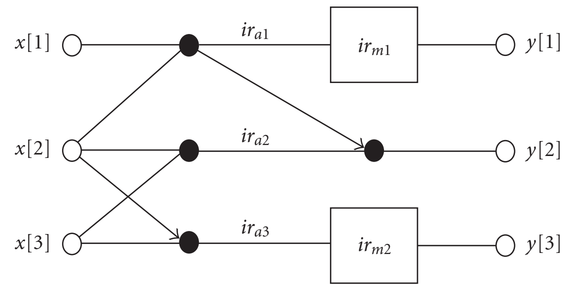

Figure 4: Exemplary butterfly structure for the computation of outputs $y[\cdot]$ based on inputs $x[\cdot]$. The data flow of DCT algorithms can be visualized using such butterfly diagrams.

such that in the next step, the coefficient is computed having the lowest computational cost. More formally, the sorted list $L = \{l_1, l_2, \ldots, l_{N^2}\}$ of coefficients l taken from an $N \times N$ DCT satisfies the condition

$$C(l_i) = \min_{k \geq i} C(l_k), \quad \forall l_i \in L \tag{4}$$

where $C(l_k)$ is a cost function providing the remaining number of operations required for the coefficient l_k given the fact that the coefficients l_n, $n < k$, already have been computed. The underlying idea is that some results of previously performed computations can be shared. Thus (4) defines a minimum computational effort needed to obtain the next coefficient.

We give a short example of how the computation order L is obtained. In Figure 4, a computation with six operation nodes is shown, where three nodes are intermediate results (ir_{a1}, ir_{a2}, and ir_{a3}). The complexity of the operations that are involved for a node can be defined such that they represent the characteristics (like CPU usage or memory access costs) of the target architecture. For this example, we assume that the nodes depicted with filled circles (•) require one operation and nodes that are depicted with squares (□) require three operations. Then, the outputs (coefficients) $y[1]$, $y[2]$, and $y[3]$ require 4, 3, and 4 operations, respectively. In this case, the first coefficient in list L is $l_1 = y[2]$ because it requires the least number of operations. Considering that, with $y[2]$, the shared node ir_1 has been computed and its intermediate result is available, the remaining coefficients $y[1]$ and $y[3]$ require 3 and 4 operations, respectively. Therefore, $l_2 = y[1]$ and $l_3 = y[3]$, leading to a computation order $L = \{y[2], y[1], y[3]\}$.

The computation order L can be perceptually optimized if the subsequent quantization step is considered. The quantizer weighting function emphasizes the use of low-frequency coefficients in the upper-left corner of the matrix. Therefore, the cost function $C(l_k)$ can be combined with a priority function to prefer those coefficients.

Note that the computation order L is determined by the algorithm and the optional applied priority function, and it can be found in advance. For this reason, no computational

	0	1	2	3	4	5	6	7
0	1	33	9	41	5	44	14	36
1	17	49	21	57	29	63	31	55
2	10	37	3	42	11	39	7	48
3	25	61	26	53	18	51	24	60
4	6	45	15	34	2	35	16	46
5	28	59	23	52	19	54	27	62
6	12	47	8	40	13	43	4	38
7	20	56	32	64	30	58	22	50

Figure 5: Computation order of coefficients.

overhead is required for actually computing the scaled DCT. It is possible, though, to apply different precomputed DCTs to different blocks employing block classification that indicates which precomputed DCT should perform best with a classified block (see Section 5.3).

4.1.3. Experiments

For experiments, the fast 2D algorithm given by Cho and Lee [9], in combination with the Arai-Agui-Nakajima (AAN) 1D algorithm [10], has been used, and this algorithm combination is extended in the following with computational complexity scalability. Both algorithms were adopted because their combination provides a highly efficient DCT computation (104 multiplications and 466 additions). The results of this experiment presented below are discussed with the assumption that an addition is equal to one operation and a multiplication is equal to three operations (in powerful cores, additions and multiplications have equal weight).

The scalability-optimized computation order in this experiment is shown in Figure 5, where the matrix has been shaded with different gray levels to mark the first and the second half of the coefficients in the sorted list. It can be seen that in this case, the computation order clearly favors horizontal or vertical edges (depending on whether the matrix is transposed or not).

Figure 6 shows the scalability of our DCT computation technique using the scalability-optimized computation order, and the zigzag order as reference computation order. In Figure 6a, it can be seen that the number of coefficients that are computed with the scalability-optimized computation order is higher at any computation limit than the zigzag order. Figure 6b shows the resulting peak signal-to-noise ratio (PSNR) of the first frame from the “Voit” sequence using both computation orders, where no quantization step is performed. A 1–5 dB improvement in PSNR can be noticed, depending on the amount of available operations.

Finally, Figure 7 shows two picture pairs (based on zigzag and scalability-optimized orders preferring horizontal details) sampled from the “Renata” sequence during different stages of the computation (representing low-cost and medium-cost applications). Perceptive evaluations of our experiments have revealed that the quality improvement of our technique is the largest between 200 and 600 operations per block. In this area, the amount of coefficients is still relatively small so that the benefit of having much more coefficients computed than in a zigzag order is fully exploited. Although the zigzag order yields perceptually important coefficients from the beginning, the computed number is simply too low to show relevant details (e.g., see the background calendar in the figure).

4.2. Scalable classification of picture blocks

4.2.1. Basics

The conventional MPEG encoding system processes each image block in the same content-independent way. However, content-dependent processing can be used to optimize the coding process and output quality, as indicated below.

(i) Block classification is used for quantization to distinguish between flat, textured, and mixed blocks [11] and then apply different quantization factors for these blocks for optimizing the picture quality at given bit rate limitations. For example, quantization errors in textured blocks have a small impact on the perceived image quality. Blocks containing both flat and textured parts (mixed blocks) are usually blocks that contain an edge, where the disturbing ringing effect gets worse with high quantization factors.

(ii) The ME (see Section 4.3) can take the advantage of classifying blocks to indicate whether a block has a structured content or not. The drawback of conventional ME algorithms that do not take the advantage of block classification is that they spend many computations on computing MVs for, for example, relatively flat blocks. Unfortunately, despite the effort, such ME processes yield MVs of poor quality. Employing block classification, computations can be concentrated on blocks that may lead to accurate MVs [12].

Of course, in order to be useful, the costs to perform block classification should be less than the saved computations. Given the above considerations, in the following, we will adopt content-dependent adaptivity for coding and motion processing. The next section explains the content adaptivity in more detail.

4.2.2. Scalability

We perform a simple block classification based on detecting horizontal and vertical transitions (edges) for two reasons.

(i) From the scalable DCT, computation orders are available that prefer coefficients representing horizontal or vertical edges. In combination with a classification, the computation order that fits best for the block content can be chosen.

(ii) The ME can be provided with the information whether it is more likely to find a good MV in up-down or left-right search directions. Since ME will find equally

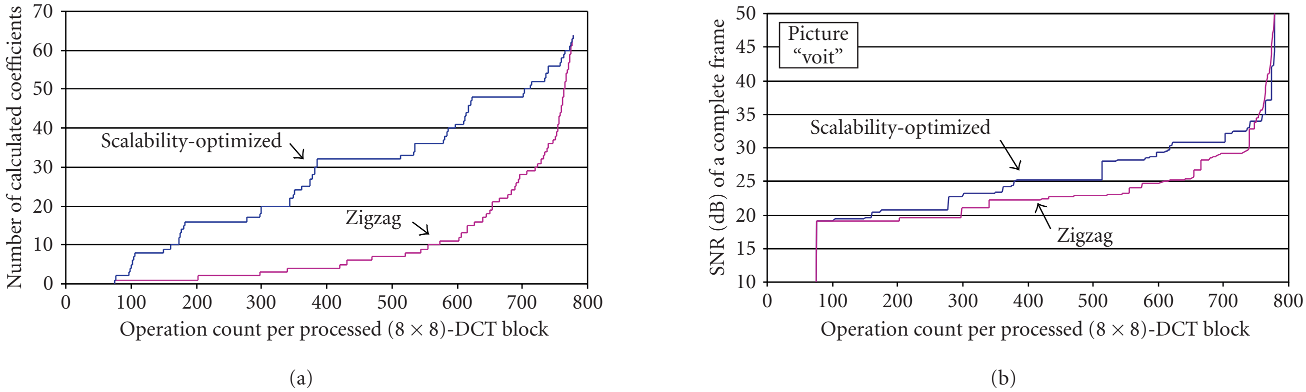

Figure 6: Comparison of the scalability-optimized computation order with the zigzag order. At limited computation resources, more DCT coefficients are computed (a) and a higher PSNR is gained (b) with the scalability-optimized order than with the zigzag order.

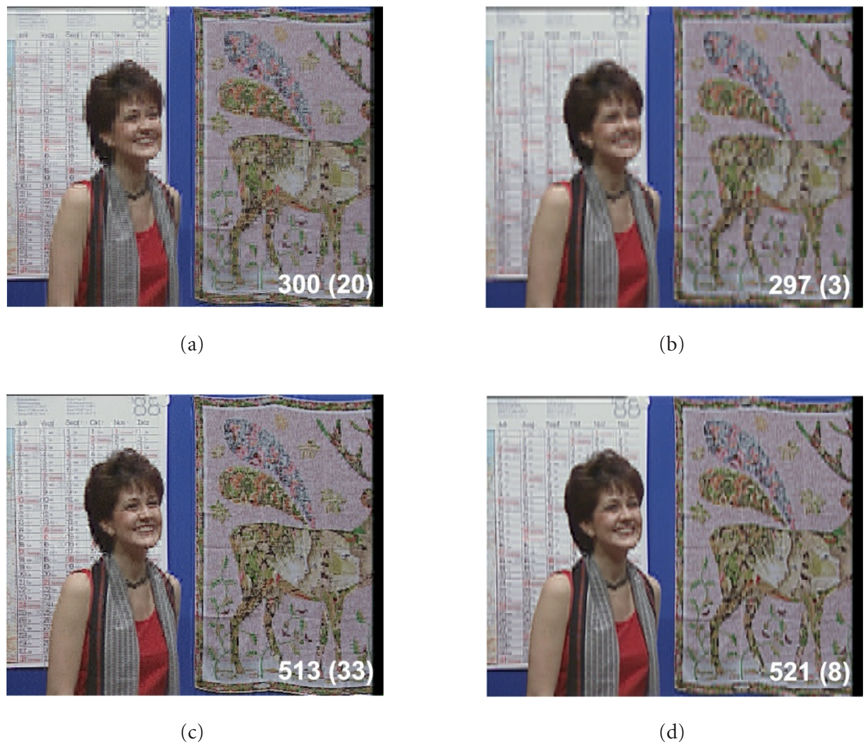

Figure 7: A video frame from the "Renata" sequence coded employing the scalability-optimized order (a) and (c), and the zigzag order (b) and (d). Index $m(n)$ means m operations are performed for n coefficients. The scalability-optimized computation order results in an improved quality (compare sharpness and readability).

good MVs for every position *along* such an edge (where a displacement in this direction does not introduce large displacement errors), searching for MVs *across* this edge will rapidly reduce the displacement error and thus lead to an appropriate MV. Horizontal and vertical edges can be detected by significant changes of pixel values in vertical and horizontal directions, respectively.

The edge detecting algorithm we use is in principle based on continuously summing up pixel differences along rows or columns and counting how often the sum exceeds a certain threshold. Let p_i, with $i = 0, 1, \ldots, 15$, be the pixel values in a row or column of a macroblock (size 16×16). We then define a range where pixel divergence (d_i) is considered as noise if $|d_i|$ is below a threshold t. The pixel divergence is defined by Table 1.

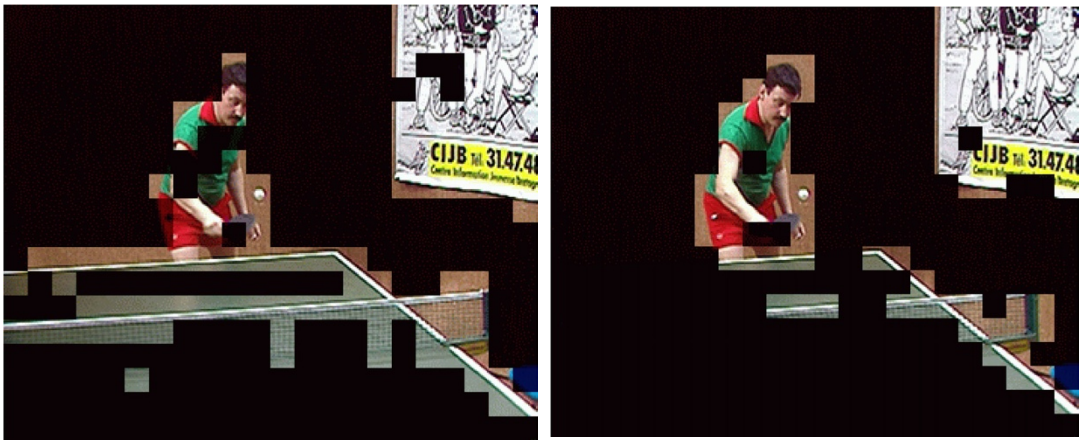

(a) (b)

Figure 8: Visualization of block classification using a picture of the "table tennis" sequence. The left (right) picture shows blocks where horizontal (vertical) edges are detected. Blocks that are visible in both pictures belong to the class "diagonal/structured," while blocks that are blanked out in both pictures are considered as "flat."

Table 1: Definition of pixel divergence, where the divergence is considered as noise if it is below a certain threshold.

Condition	Pixel divergence d_i
$i = 0$	0
$(i = 1, \dots, 15) \wedge (\lvert d_{i-1} \rvert \le t)$	$d_{i-1} + (p_i - p_{i-1})$
$(i = 1, \dots, 15) \wedge (\lvert d_{i-1} \rvert > t)$	$d_{i-1} + (p_i - p_{i-1}) - \operatorname{sgn}(d_{i-1}) * t$

The area preceding the edge yields a level in the interval $[-t; +t]$. The middle of this interval is at $d = 0$, which is modified by adding $\pm t$ in the case that $|d|$ exceeds the interval around zero (start of the edge). This mechanism will follow the edges and prevent noise from being counted as edges. The counter c as defined below indicates how often the actual interval was exceeded:

$$c = \sum_{i=1}^{15} \begin{cases} 0 & \text{if } |d_i| \le t, \\ 1 & \text{if } |d_i| > t. \end{cases} \tag{5}$$

The occurrence of an edge is defined by the resulting value of c from (5).

This edge detecting algorithm is scalable by selecting the threshold t, the number of rows and columns that are considered for the classification, and a typical value for c. Experimental evidence has shown that in spite of the complexity scalability of this classification algorithm, the evaluation of a single row or column in the middle of a picture block was found sufficient for a rather good classification.

4.2.3. Experiments

Figure 8 shows the result of an example to classify image blocks of size 16×16 pixels (macroblock size). For this experiment, a threshold of $t = 25$ was used. We considered a block to be classified as a "horizontal edge" if $c \ge 2$ holds for the central column computation and as a "vertical edge" if $c \ge 2$ holds for the row computation. Obviously, we can derive two extra classes: "flat" (for all blocks that do not belong to the CLASS "horizontal edge" NOR the class "vertical edge") and diagonal/structured (for blocks that belong to both classes horizontal edge and vertical edge).

The visual results of Figure 8 are just an example of a more elaborate set of sequences with which experiments were conducted. The results showed clearly that the algorithm is sufficiently capable of classifying the blocks for further content-adaptive processing.

4.3. Motion estimation

4.3.1. Basics

The ME process in MPEG systems divides each frame into rectangular macroblocks (16×16 pixels each) and computes MVs per block. An MV signifies the displacement of the block (in the x-y pixel plane) with respect to a reference image. For each block, a number of candidate MVs are examined. For each candidate, the block evaluated in the current image is compared with the corresponding block fetched from the reference image displaced by the MV. After testing all candidates, the one with the best match is selected. This match is done on basis of the SAD between the current block and the displaced block. The collection of MVs for a frame forms an MV field.

State-of-the-art ME algorithms [13, 14, 15] normally concentrate on reducing the number of vector candidates for a single-sided ME between two frames, independent of the frame distance. The problem of these algorithms is that a higher frame distance hampers accurate ME.

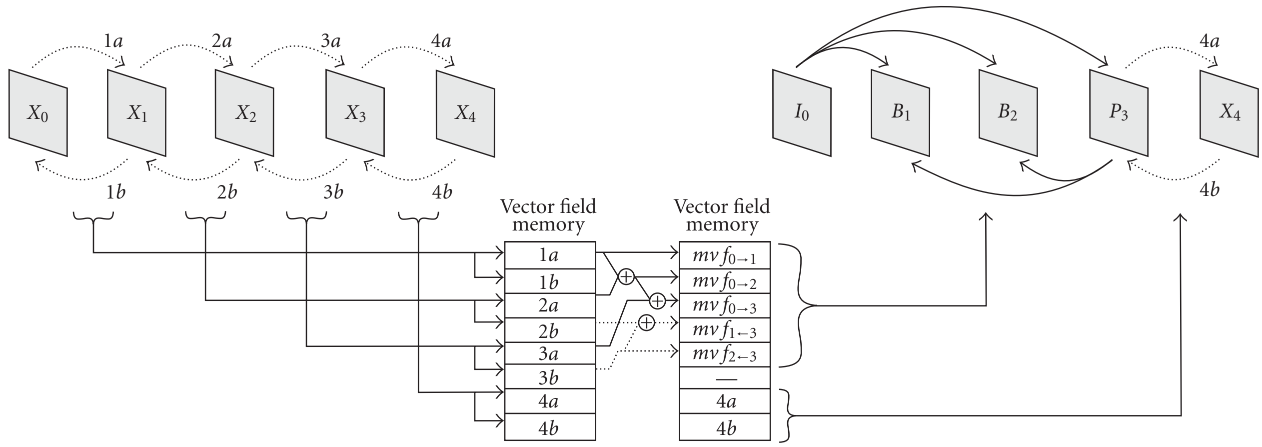

Figure 9: An overview of the new scalable ME process. Vector fields are computed for successive frames (left) and stored in memory. After defining the GOP structure, an approximation is computed (middle) for the vector fields needed for MPEG coding (right). Note that for this example it is assumed that the approximations are performed after the exemplary GOP structure is defined (which enables dynamic GOP structures), therefore the vector field ($1b$) is computed but not used afterwards. With predefined GOP structures, the computation of ($1b$) is not necessary.

4.3.2. Scalability

The scalable ME is designed such that it takes the advantage of the intrinsically high prediction quality of ME between successive frames (smallest temporal distance), and thereby works not only for the typical (predetermined and fixed) MPEG GOP structures, but also for more general cases. This feature enables on-the-fly selection of GOP structures depending on the video content (e.g., detected scene changes, significant changes of motion, etc.). Furthermore, we introduce a new technique for generating MV fields from other vector fields by *multitemporal* approximation (not to be confused with other forms of multitemporal ME as found in H.264). These new techniques give more flexibility for a scalable MPEG encoding process.

The estimation process is split up into three stages as follows.

Stage 1 Prior to defining a GOP structure, we perform a simple recursive motion estimation (RME) [16] for every received frame to compute the forward and backward MV field between the received frame and its predecessor (see the left-hand side of Figure 9). The computation of MV fields can be omitted for reducing computational effort and memory.

Stage 2 After defining a GOP structure, all the vector fields required for MPEG encoding are generated through multitemporal approximations by summing up vector fields from the previous stage. Examples are given in the middle of Figure 9, for example, vector field $(mv\, f_{0\to3}) = (1a) + (2a) + (3a)$. Assume that the vector field ($2a$) has not been computed in Stage 1 (due to a chosen scalability setting), one possibility to approximate $(mv\, f_{0\to3})$ is $(mv\, f_{0\to3}) = 2 * (1a) + (3a)$.

Stage 3 For final MPEG ME in the encoder, the computed approximated vector fields from the previous stage are used as an input. Beforehand, an optional refinement of the approximations can be performed with a second iteration of simple RME.

We have employed simple RME as a basis for introducing scalability because it offers a good quality for time-consecutive frames at low computing complexity.

The presented three-stage ME algorithm differs from known multistep ME algorithms like in [17], where initially estimated MPEG vector fields are processed for a second time. Firstly, we do not have to deal with an increasing temporal distance when deriving MV fields in Stage 1. Secondly, we process the vector fields in a display order having the advantage of frame-by-frame ME, and thirdly, our algorithm provides scalability. The possibility of scaling vector fields, which is part of our multitemporal predictions, is mentioned in [17] but not further exploited. Our algorithm makes explicit use of this feature, which is a fourth difference. In the sequel, we explain important system aspects of our algorithm.

Figure 10 shows the architecture of the three-stage ME algorithm embedded in an MPEG encoder. With this architecture, the initial ME process in Stage 1 results in a high-quality prediction because original frames without quantization errors are used. The computed MV fields can be used in Stage 2 to optimize the GOP structures. The optional refinement of the vector fields in Stage 3 is intended for high-quality applications to reach the quality of a conventional MPEG ME algorithm.

The main advantage of the proposed architecture is that it enables a broad scalability range of resource usage and achievable picture quality in the MPEG encoding process. Note that a bidirectional ME (usage of B-frames) can be realized at the same cost of a single-directional ME (usage of P-frames only) when properly scaling the computational

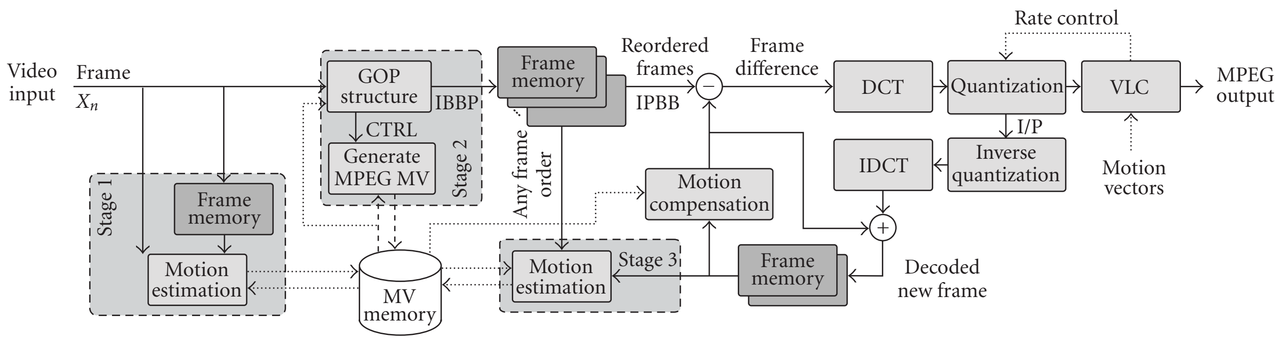

Figure 10: Architecture of an MPEG encoder with the new scalable three-stage motion estimation.

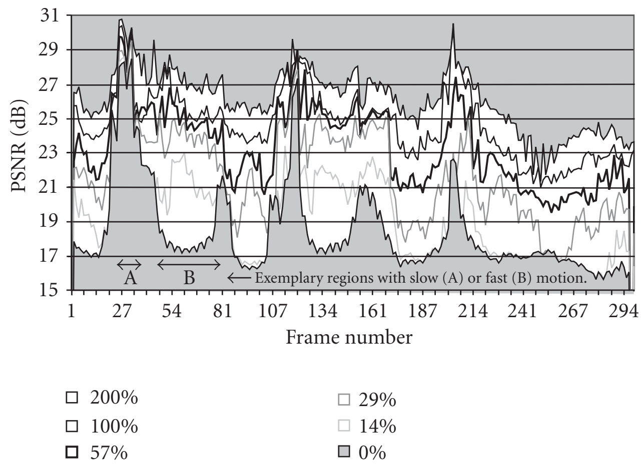

Figure 11: PSNR of motion-compensated B-frames of the "Stefan" sequence (tennis scene) at different computational efforts—P-frames are not shown for the sake of clarity ($N = 16$, $M = 4$). The percentage shows the different computational effort that results from omitting the computation of vector fields in Stage 1 or performing an additional refinement in Stage 3.

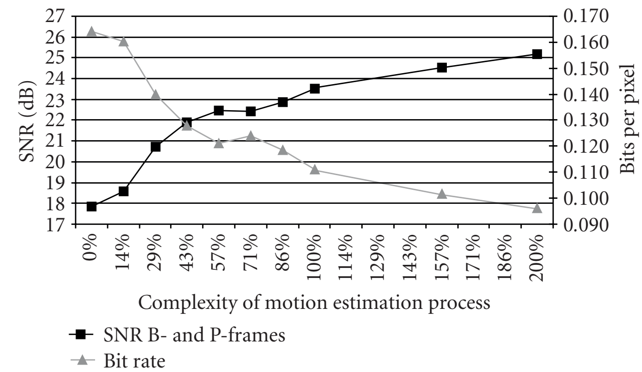

Figure 12: Average PSNR of motion-compensated P- and B-frames and the resulting bit rate of the encoded "Stefan" stream at different computational efforts. A lower average PSNR results in a higher differential signal that must be coded, which leads to a higher bit rate. The percentage shows the different computational effort that results from omitting the computation of vector fields in Stage 1 or performing an additional refinement in Stage 3.

complexity, which makes it affordable for mobile devices that up till now rarely make use of B-frames. A further optimization is seen (but not worked out) in limiting the ME process of Stages 1 and 3 to significant parts of a vector field in order to further reduce the computational effort and memory.

4.3.3. Experiments

To demonstrate the flexibility and scalability of the three-stage ME technique, we conducted an initial experiment using the "Stefan" sequence (tennis scene). A GOP size of $N = 16$ and $M = 4$ (thus "IBBBP" structure) was used, combined with a simple pixel-based search. In this experiment, the scaling of the computational complexity is introduced by gradually increasing the vector field computations in Stage 1 and Stage 3. The results of this experiment are shown in Figure 11. The area in the figure with the white background shows the scalability of the quality range that results from downscaling the amount of computed MV fields. Each vector field requires 14% of the effort compared to a 100% simple RME [16] based on four forward vector fields and three backward vector fields when going from one to the next reference frame. If all vector fields are computed and the refinement Stage 3 is performed, the computational effort is 200% (not optimized).

The average PSNR of the motion-compensated P- and B-frames (taken after MC and before computing the differential signal) of this experiment and the resulting bit rate of the encoded MPEG stream are shown in Figure 12. Note that for comparison purpose, no bit rate control is performed during encoding and therefore, the output quality of the MPEG streams for all complexity levels is equal. The quantization factors, *qscale*, we have used are 12 for I-frames and 8 for P- and B-frames. For a full quality comparison (200%), we consider a full-search block matching with a search window of 32×32 pixels. The new ME technique slightly outperforms this full search by 0.36 dB PSNR measured from the motion-compensated P- and B-frames of this experiment (25.16 dB instead of 24.80 dB). The bit rate of the complete MPEG

Table 2: Average luminance PSNR of the motion-compensated P- and B-frames for sequences "Stefan" (A), "Renata" (B), and "Teeny" (C) with different ME algorithms. The second column shows the average number of SAD-based vector evaluations per MV (based on (A)).

Algorithm	Tests/MV	(A)	(B)	(C)
2D FS (32 × 32)	926.2	24.80	29.62	26.78
NTSS [14]	25.2	22.55	27.41	24.22
Diamond [15]	21.9	22.46	27.34	26.10
Simple RME [16]	16.0	21.46	27.08	23.89
Three-stage ME 200% (employing [16])	37.1	25.16	29.24	26.92
Three-stage ME 100% (employing [16])	20.1	23.52	27.45	24.74

sequence is 0.012 bits per pixel (bpp) lower when using the new technique (0.096 bpp instead of 0.108 bpp). When reducing the computational effort to 57% of a single-pass simple RME, an increase of the bit rate by 0.013 bpp compared to the 32 × 32 full search (FS) is observed.

Further comparisons are made with the scalable three-stage ME running at full and "normal" quality. Table 2 shows the average PSNR of the motion-compensated P- and B-frames for three different video sequences and ME algorithms with the same conditions as described above (same N, M, etc.). The first data column (tests per MV) shows the average number of vector tests that are performed per macroblock in the "Stefan" sequence to indicate the performance of the algorithms. Note that MV tests pointing outside the picture are not counted, which results in numbers that are lower than the nominal values (e.g., 926.2 instead of 1024 for 32 × 32 FS). The simple RME algorithm results in the lowest quality here because only three vector field computations out of $4 * (4 + 3) = 28$ can use temporal vector candidates as prediction. However, our new three-stage ME that uses this simple RME performs, comparable to FS, at 200% complexity, and at 100%, it is comparable to the other fast ME algorithms.

The results in Table 2 are based on the simple RME algorithm from [16]. A modified algorithm has been found later [18] that forms an improved replacement for the simple RME. This modified algorithm is based on the block classification as presented in Section 4.2. This algorithm was used for further experiments and is summarized as follows. Prior to estimating the motion between two frames, the macroblocks inside a frame are classified into areas having horizontal, vertical edges, or no edges. The classification is exploited to minimize the number of MV evaluations for each macroblock by, for example, concentrating vector evaluations across the detected edge. A novelty in the algorithm is a *distribution* of good MVs *to* other macroblocks, even already processed ones, which differs from other known recursive ME techniques that reuse MVs *from previously* processed blocks.

5. SYSTEM ENHANCEMENTS AND EXPERIMENTS

The key approach to optimize a system is to reuse and combine data that is generated by the system modules in order to control other modules. In the following, we present several approaches, where data can be reused or generated at a low cost in a coding system for an optimization purpose.

5.1. Experimental environment

The scalable modules for the (I)DCT, (de)quantization, ME, and VLC are integrated into an MPEG encoder framework, where the scaling of the IDCT and the (de)quantization is effected from the scalable DCT (see Section 5.2). In order to visualize the obtained scalability of the computations, the scalable modules are executed at different parameter settings, leading to effectively varying the number of DCT coefficients and MV candidates evaluated. When evaluating the system complexity, the two different numbers have to be combined into a joint measure. In the following, the elapsed execution time of the encoder needed to code a video sequence is used as a basis for comparison. Although this time parameter highly depends on the underlying architecture and on the programming and operating system, it reflects the complexity of the system due to the high amount of operations involved.

The experiments were conducted on a Pentium-III Linux system running at 733 MHz. In order to be able to measure the execution time of single functions being part of the complete encoder execution, it was necessary to compile the C++ program of the encoder without compiler optimizations. Additionally, it should be noted that the experimental C++ code was not optimized for fast execution or usage of architecture-specific instructions (e.g., MMX). For these reasons, the encoder and its measured execution times cannot be compared with existing software-based MPEG encoders. However, we have ensured that the measured change in the execution time results from the scalability of the modules, as we did not change the programming style, code structures, or common coding parameters.

5.2. Effect of scalable DCT

The fact that a scaled DCT computes only a subset S of all possible DCT coefficients C can be used for the optimization of other modules. The subset S is known before the subsequent quantization, dequantization, VLC, and IDCT modules. Of course, coefficients that are not computed are set to zero and therefore they do not have to be processed further in any of these modules. Note that because the subset S is known in advance, no additional tests are performed to

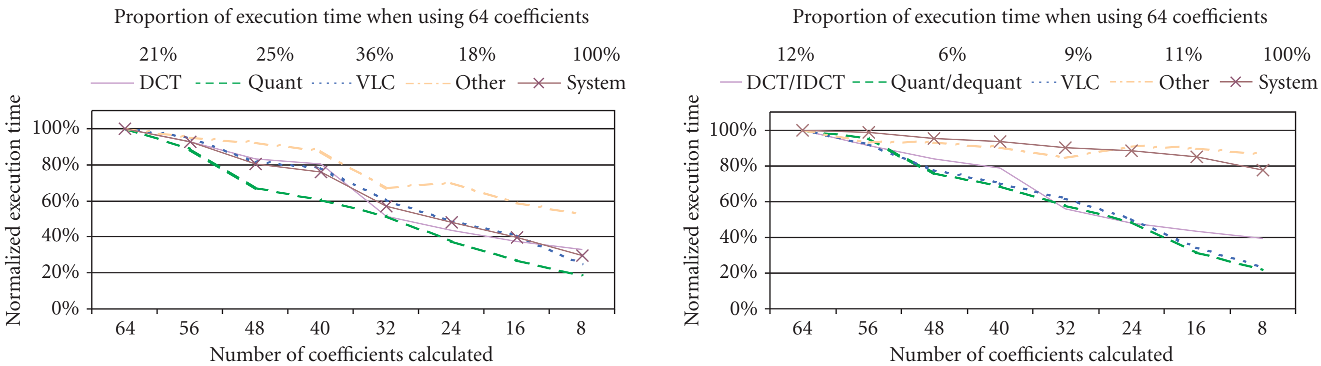

(a) (1,1)-GOP (I-frames only).

(b) (12,4)-GOP (IBBBP structure).

Figure 13: Complexity reduction of the encoder modules relative to the full DCT processing, with (1,1)-GOPs (a) and with (12,4)-GOPs) (b). Note that in this case, 62% of the coding time is spent in (b) for ME and MC (not shown for convenience). For visualization of the complexity reduction, we normalize the execution time for each module to 100% for full processing.

detect zero coefficients. This saves computations as follows.

(i) The quantization and dequantization require a fixed amount of operations per processed intra- or intercoefficient. Thus, each skipped coefficient $c \in C \setminus S$ saves 1/64 of the total complexity of the quantization and dequantization modules.

(ii) The VLC processes the DCT coefficients in a zigzag or an alternate order and generates run-value pairs for coefficients that are unequal to zero. "Run" indicates the number of zero coefficients that are skipped before reaching a nonzero coefficient. The usage of a scaled DCT increases the probability that zero coefficients occur, for which no computations are spent.

(iii) The IDCT can be simplified by knowing which coefficients are zero. It is obvious that, for example, each multiplication with a known factor of 0 and additions with a known addend of 0 can be skipped.

The execution time of the modules when coding the "Stefan" sequence and scaling the modules that process coefficients is visualized in Figure 13. The category "other" is used for functions that are not exclusively used by the scaled modules. Figure 13a shows the results of an experiment, where the sequence was coded with I-frames only. Similar results are observed in Figure 13b from another experiment, for which P- and B-frames are included. To remove the effect of quantization, the experiments were performed with qscale = 1. In this way, the figures show results that are less dependent on the coded video content.

The measured PSNR of the scalable encoder running at full quality is 46.5 dB for Figure 13a and 48.16 dB for Figure 13b. When the number of computed coefficients is gradually reduced from 64 to 8, the PSNR drops gradually to 21.4 dB Figure 13a, respectively, 21.81 dB in Figure 13b. In Figures 13a and 13b, the quality gradually reduces from "no noticeable differences" down to "severe blockiness." In Figure 13b, the curve for the ME module is not shown for convenient because the ME (in this experiment, we used diamond search ME [15]) is not affected from processing a different number of DCT coefficients.

5.3. Selective DCT computation based on block classification

The block classification introduced in Section 4.2 is used to enhance the output quality of the scaled DCT by using different computation orders for blocks in different classes. A simple experiment indicates the benefit in quality improvement. In the experiment, we computed the average values of DCT coefficients when coding the "table tennis" sequence with I-frames only. Each DCT block is taken after quantization with qscale = 1. Figure 14 shows the statistic for blocks that are classified as having a horizontal (left graph) or vertical (right graph) edge only. It can be seen that the classification leads to a frequency concentration in the DCT coefficient matrix in the first column, respectively, row.

We found that the DCT algorithm of Arai et al. [10] can be used best for blocks with horizontal or vertical edges, while background blocks have a better quality impression when using the algorithm by Cho and Lee [9]. The experiment made for Figure 15 shows the effect of the two algorithms on the table edges ([10] is better) and the background ([9] is better). In both cases, the computation orders designed for preferring horizontal edges are used. The computation limit was set to 256 operations, leading to 9 computed coefficients for [10] and 11 for [9], respectively. The coefficients that are computed are marked in the corresponding DCT matrix. It can be seen that [10] covers all main vertical frequencies, while [9] covers a mixture of high and low vertical and horizontal frequencies. The resulting overall PSNR are 26.58 dB and 24.32 dB, respectively.

Figure 16 shows the effect of adaptive DCT computation based on classification. Almost all of the background blocks were classified as flat blocks and therefore, ChoLee was chosen for these blocks. For convenient, both algorithms were set

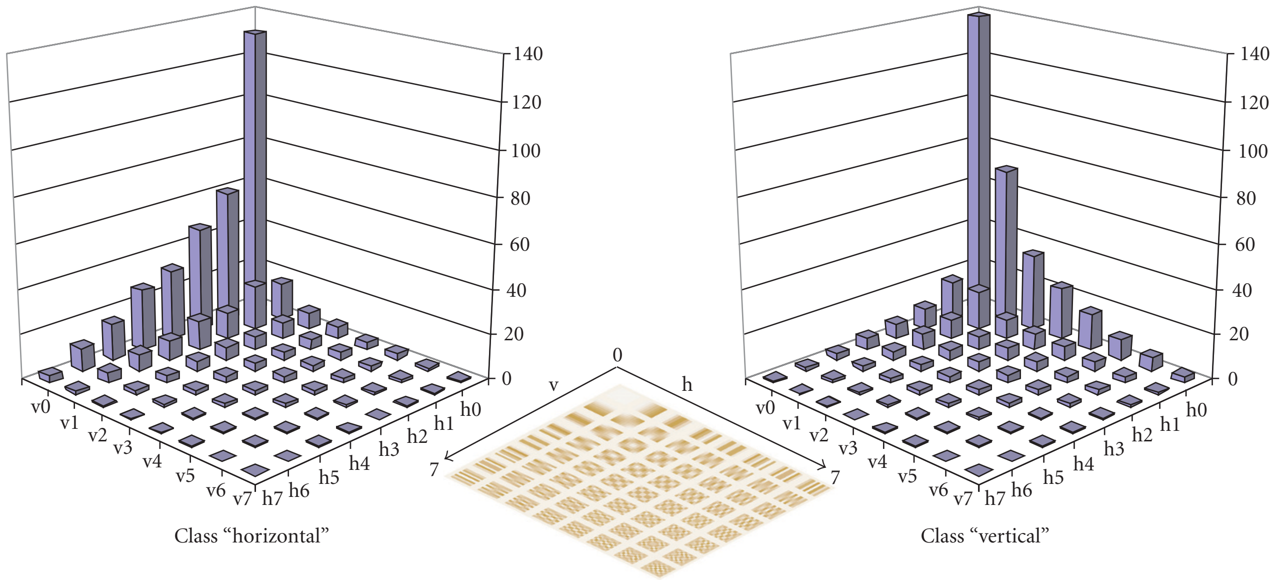

Figure 14: Statistics of the average absolute values of the DCT coefficients taken after quantization with qscale = 1. Here, the "table tennis" sequence was coded with I-frames only. The left (right) graph shows the statistic for blocks classified as having horizontal (vertical) edges.

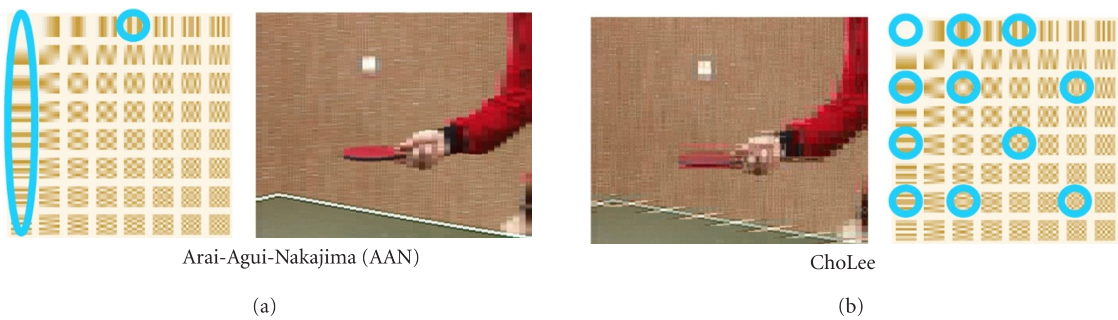

Figure 15: Example of scaled AAN-DCT (a) and ChoLee-DCT (b) at 256 operations. AAN fits better for horizontal edges, while ChoLee has better results for the background.

to compute 11 coefficients. Blocks with both detected horizontal and vertical edges are treated as blocks having horizontal edges only because an optimized computation order for such blocks is not yet defined. The resulting PSNR is 26.91 dB.

5.4. *Dynamic interframe DCT coding*

Besides intraframe coding, the DCT computation on frame differences (for interframe coding) occurs more often than intraframe coding ($N - 1$ times for (N, M) GOPs). For this reason, we look more closely to interframe DCT coding, where we discovered a special phenomenon from the scalable DCT. It was found that the DCT coded frame differences show temporal fluctuations in frequency content. The temporal fluctuation is caused by the motion in the video content combined with the special selection function of the coefficients computed in our scalable DCT. Due to the motion, the energy in the coefficients shifts over the selection pattern so that the quality gradually increases over time. Figure 17 shows this effect from an experiment when coding the "Stefan" sequence with IPP frames (GOP structure (GOP size N, IP distance M) $= (12, 1)$) while limiting the computation to 32 coefficients. The camera movement in the shown sequence is panning to the right. It can be seen for example that the artifacts around text decrease over time.

The aforementioned phenomenon was mainly found in sequences containing not too much motion. The described effect leads to the idea of temporal data partitioning using a cyclical sequence of several scalable DCTs with different coefficient selection functions. The complete cycle would compute each coefficient at least once. Temporal data partitioning means that the computational complexity of the DCT computation is spread over time, thereby reducing the average complexity of the DCT computation (per block) at the expense of obtaining delayed quality obtainment. Using this technique, picture blocks having a static content (blocks

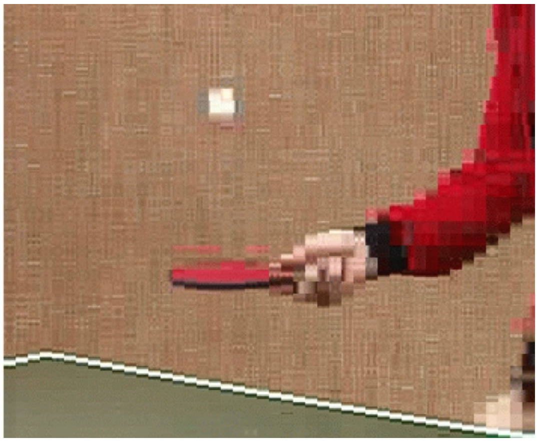

Figure 16: Both DCT algorithms were used to code this frame. After block classification, the ChoLee-DCT was used to code blocks where no edges were detected and the AAN-DCT for blocks with detected edges.

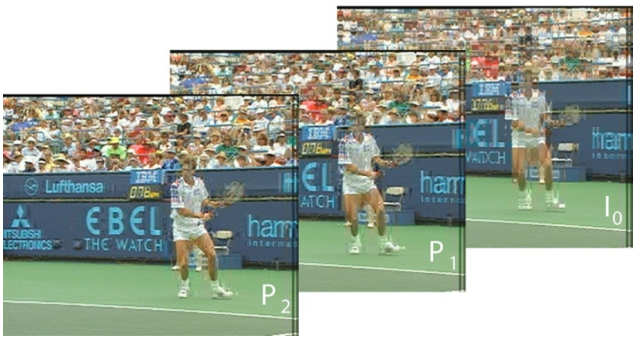

Figure 17: Visualization of a phenomenon from the scalable DCT, leading to a gradual quality increase over time.

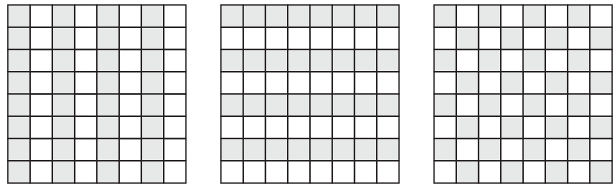

Figure 18: Example of coefficient subsets (marked gray) used for dynamic interframe DCT coding with a limitation to 32 coefficients per subset.

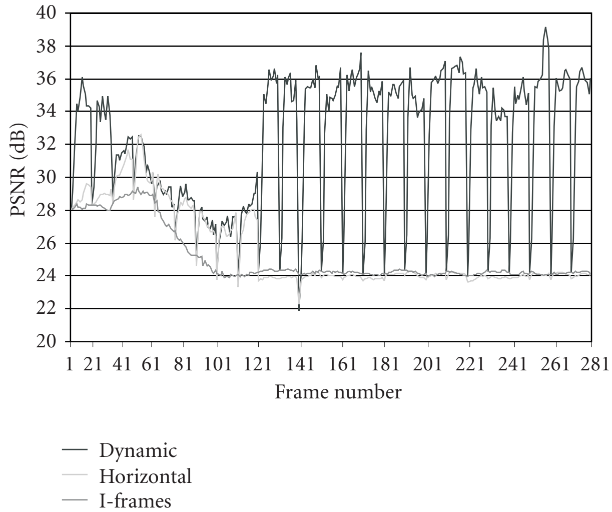

Figure 19: PSNR measures for the coded "table tennis" sequence, where the DCT computation was scaled to compute 32 coefficients. Compared to coding I-frames only (medium gray curve), inter DCT coding results in an improved output quality in case of motion (light gray curve) and even a higher output quality with dynamic interframe DCT computation.

having zero motion like nonmoving background) and therefore having no temporal fluctuations in their frequency content will obtain the same result as a nonpartitioned DCT computation after full computation of the partitioned DCT.

Based on the idea of temporal data partitioning, we define N subsets s_i (with $i = 0, \ldots, N-1$) of coefficients such that

$$\bigcup_{i=0}^{N-1} s_i = S, \tag{6}$$

where the set S contains all the 64 DCT coefficients. The subsets s_i are used to build up functions f_i that compute a scaled DCT for the coefficients in s_i. The functions f_i are applied to blocks with static contents in cyclical sequence (one per intercoded frame). After N intercoded frames, each coefficient for these blocks is computed at least once.

We set up an experiment using the "table tennis" sequence as follows in order to measure the effect of dynamic interframe coding. The computation of the DCT (for intraframe coding and interframe coding) was limited to 32 coefficients. The coefficient subsets we used are shown in Figure 18. Figure 19 shows the improvement in the PSNR that is achieved with this approach. Three curves are shown in this figure, plotting the achieved PSNR of the coded frames. The medium gray curve results from coding all the frames as I-frames, which we take as a reference in this experiment. The other two curves result from applying a GOP structure with $N = 16$ and $M = 4$. First, all blocks are processed with a fixed DCT (light gray curve) computing only the coefficients as shown in the left subset of Figure 18. It can be seen that when the content of the sequence changes due to movement, the PSNR increases. Second, the dynamic inter-DCT coding technique is applied to the coding process, which results in the dark gray curve. The dark gray curve shows an improvement to the light gray curve in case of no motion. The comb-like structure of the curve results from the periodic I-frame occurrence that restarts the quality buildup. The low periodicity of the quality drop gives a visually annoying effect that can be solved by computing more

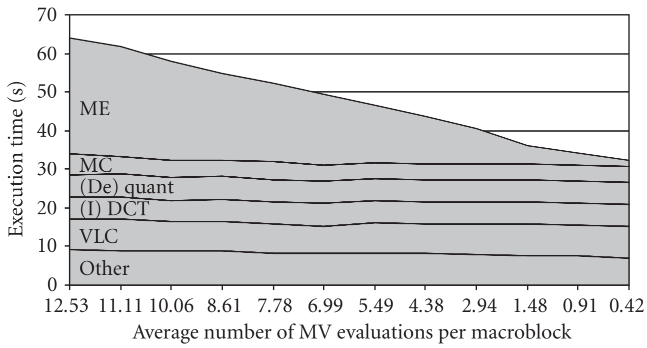

Figure 20: Example of ME scalability for the complete encoder when using a (12, 4)-GOP ("IBBBP" structure) for coding.

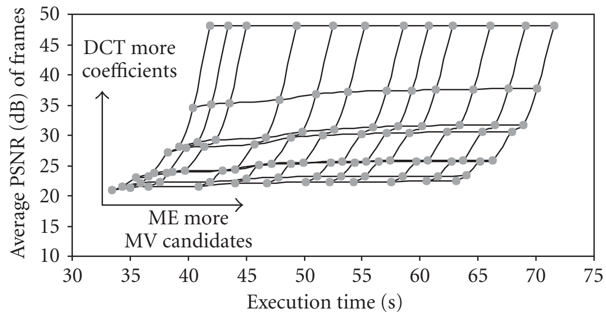

Figure 21: PSNR results of different configurations for the scalable MPEG modules.

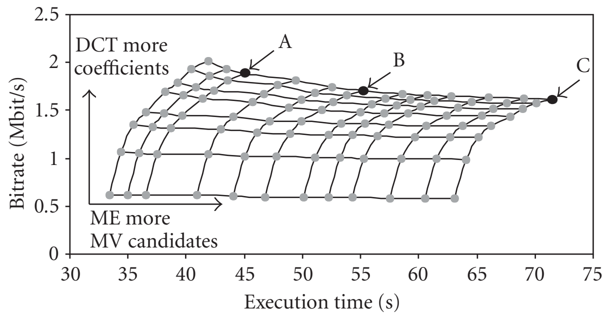

Figure 22: Obtained bit rates of different configurations for the scalable modules. The markers refer to points in the design space, where the same bit rate and quality (not computational complexity) is obtained as resulting from using diamond search (A) or full search with a 32 × 32 (B) or 64 × 64 (C) search area for ME.

coefficients for the I-frames. Although this seems interesting, this was not further pursued because of limited time.

5.5. *Effect of scalable ME*

The execution time of the MPEG modules when coding the "Stefan" sequence and scaling the ME is visualized in Figure 20. It can be seen that the curve for the ME block scales linearly with the number of MV evaluations, whereas the other processing blocks remain constant. The average number of vector candidates that are evaluated per macroblock by the scalable ME in this experiment is between 0.42 and 12.53. This number is clearly below the achieved average number of candidates (21.77) when using the diamond search [15]. At the same time, we found that our scalable codec results in a higher quality of the MC frame (up to 25.22 dB PSNR in average) than the diamond search (22.53 dB PSNR in average), which enables higher compression ratios (see the next section).

5.6. *Combined effect of scalable DCT and scalable ME*

In this section, we combine the scalable ME and DCT in the MPEG encoder and apply the scalability rules for (de)quantization, IDCT, and VLC, as we have described them in Section 2. Since the DCT and ME are the main sources for scalability, we will focus on the tradeoff between MVs and the number of computed coefficients.

Figure 21 portrays the obtained average PSNR of the coded "Stefan" sequence (CIF resolution) and Figure 22 shows the achieved bit rate corresponding to Figure 21. The experiments are performed with a (12,4)-GOP and qscale = 1. Both figures indicate the large design space that is available with the scalable encoder without quantization and open-loop control. The horizontally oriented curves refer to a fixed number of DCT coefficients (e.g., $8, 16, 24, 32, \ldots, 64$), whereas vertically oriented curves refer to a fixed number of MV candidates. A normal codec would compute all the 64 coefficients and would therefore operate on the top horizontal curve of the graph. The figures should be jointly evaluated. Under the above-mentioned measurement conditions, the potential benefit of the scalable ME is only visible in the reduction of the bit rate (see Figure 22) since an improved ME leads to less DCT coefficients for coding the difference signal after the MC in the MPEG loop.

In Figure 22, it can be seen that the bit rate decreases when computing more MV candidates (going to the right). The reduction is only visible when the bit rate is high enough. For comparison, the markers "A," "B", and "C" refer to three points from the design space. With these markers, the obtained bit rate of the scalable encoder is compared to the encoder using another ME algorithm. Marker "A" refers to the configuration of the encoder using the scalable ME, where the same bit rate and video quality (not the computational complexity) are achieved compared to the diamond search. As mentioned earlier, the diamond search performs 21.77 MV candidates on the average per macroblock. Our scalable coder operating under the same quality and bit rate combination as the diamond search in marker "A" results in 10.06 average MV candidates, thus 53.8% less than the diamond search. Markers "B" and "C" result from using the full-search ME with a 32 × 32 and 64 × 64 search area, respectively, requiring substantially more vector candidates (1024 and 4096, respectively). Figure 21 shows a corresponding measurement with the average PSNR, as the outcome, instead of the bit rate.

Figures 21 and 22 both present a large design space, but in practice, this is limited due to the quantization and bit rate control. Further experiments using quantization and bit rate control at 1500 kbps for the "Stefan," "Foreman," and "table tennis" sequence resulted in a quality level range from roughly 22 dB to 38 dB. As could be expected from inserting the quantization, the curves moved to lower PSNR (the lower half of Figure 21) and less computation time is required since fewer coefficients are computed. It was found that the remaining design space is larger for sequences having less motion.

6. CONCLUSIONS

We have presented techniques for complexity scalable MPEG encoding that gradually reduce the quality as a function of limited resources. The techniques involve modifications to the encoder modules in order to pursue scalable complexity and/or quality. Special attention has been paid to exploiting a scalable DCT and ME because they represent two computational expensive corner stones of MPEG encoding. The introduced new techniques for the scalability of the two functions show considerable savings of computational complexity for video applications having low-quality requirements. In addition, a scalable block classification technique has been presented, which is designed to support the scalable processing of the DCT and ME. In the second step, performance evaluations have been carried out by constructing a complete MPEG encoding system in order to show the design space that is achieved with the scalability techniques. It has been shown that even a higher reduction in computational complexity of the system could be obtained if available data (e.g., which DCT coefficients are computed during a scalable DCT computation) is exploited to optimize other core functions.

The obtained execution times of the encoder when coding the "Stefan" sequence as an example for complexity has been measured. It was found that the overall execution time of the scalable encoder can be gradually reduced to roughly 50% of its original execution time. At the same time, the codec provides a wide range of video quality levels (roughly from 20 dB to 48 dB PSNR in average) and compression ratios (from 0.58 to 2.02 Mbps). Further experiments targeting a bit rate of 1500 kbps for the Stefan, Foreman, and table tennis sequence result in a quality level range from roughly 21.5 dB to 38.5 dB. Compared with the diamond search ME from literature which requires 21.77 MV candidates on the average per macroblock, our scalable coder operating under the same quality and bit rate combination uses 10.06 average MV candidates, thus 53.8% less than the diamond search.

Another result of our experiments is that the scalable DCT has an integrated coefficient selection function which may enable a quality increase during interframe coding. This phenomenon can lead to an MPEG encoder with a number of special DCTs with different selection functions, and this option should be considered for future work. This should also include different scaling of the DCT for intra- and interframe coding. For scalable ME, future work should examine the scalability potentials of using various fixed and dynamic GOP structures, and of concentrating or limiting the ME to frame parts, whose content (could) have the current viewer focus.

REFERENCES

[1] C. Hentschel, R. Braspenning, and M. Gabrani, "Scalable algorithms for media processing," in *IEEE International Conference on Image Processing (ICIP '01)*, vol. 3, pp. 342–345, Thessaloniki, Greece, October 2001.

[2] R. Prasad and K. Ramkishor, "Efficient implementation of MPEG-4 video encoder on RISC core," in *IEEE International Conference on Consumer Electronics, Digest of Technical papers (ICCE '02)*, pp. 278–279, Los Angeles, Calif, USA, June 2002.

[3] K. Lengwehasatit and A. Ortega, "DCT computation based on variable complexity fast approximations," in *Proc. IEEE International Conference of Image Processing (ICIP '98)*, vol. 3, pp. 95–99, Chicago, Ill, USA, October 1998.

[4] S. Peng, "Complexity scalable video decoding via IDCT data pruning," in *International Conference on Consumer Electronics (ICCE '01)*, pp. 74–75, Los Angeles, Calif, USA, June 2001.

[5] Y. Chen, Z. Zhong, T. H. Lan, S. Peng, and K. van Zon, "Regulated complexity scalable MPEG-2 video decoding for media processors," *IEEE Trans. Circuits and Systems for Video Technology*, vol. 12, no. 8, pp. 678–687, 2002.

[6] R. Braspenning, G. de Haan, and C. Hentschel, "Complexity scalable motion estimation," in *Proc. of SPIE: Visual Communications and Image Processing 2002*, vol. 4671, pp. 442–453, San Jose, Calif, USA, 2002.

[7] S. Mietens, P. H. N. de With, and C. Hentschel, "New DCT computation technique based on scalable resources," *Journal of VLSI Signal Processing Systems for Signal, Image, and Video Technology*, vol. 34, no. 3, pp. 189–201, 2003.

[8] S. Mietens, P. H. N. de With, and C. Hentschel, "Frame reordered multi-temporal motion estimation for scalable MPEG," in *Proc. 23rd International Symposium on Information Theory in the Benelux*, Louvain-la-Neuve, Belgium, May 2002.

[9] N. Cho and S. Lee, "Fast algorithm and implementation of 2-D discrete cosine transform," *IEEE Trans. Circuits and Systems*, vol. 38, no. 3, pp. 297–305, 1991.

[10] Y. Arai, T. Agui, and M. Nakajima, "A fast DCT-SQ scheme for images," *Transactions of the Institute of Electronics, Information and Communication Engineers*, vol. 71, no. 11, pp. 1095–1097, 1988.

[11] D. Farin, N. Mache, and P. H. N. de With, "A software-based high-quality MPEG-2 encoder employing scene change detection and adaptive quantization," *IEEE Transactions on Consumer Electronics*, vol. 48, no. 4, pp. 887–897, 2002.

[12] T. Kummerow and P. Mohr, *Method of determining motion vectors for the transmission of digital picture information*, EPO 496 051, European Patent Application, November 1991.

[13] M. Chen, L. Chen, and T. Chiueh, "One-dimensional full search motion estimation algorithm for video coding," *IEEE Trans. Circuits and Systems for Video Technology*, vol. 4, no. 5, pp. 504–509, 1994.

[14] R. Li, B. Zeng, and M. Liou, "A new three-step search algorithm for block motion estimation," *IEEE Trans. Circuits and Systems for Video Technology*, vol. 4, no. 4, pp. 438–442, 1994.

[15] J. Tham, S. Ranganath, M. Ranganath, and A. A. Kassim, "A novel unrestricted center-biased diamond search algorithm for block motion estimation," *IEEE Trans. Circuits and Systems for Video Technology*, vol. 8, no. 4, pp. 369–377, 1998.

[16] P. N. H. de With, "A simple recursive motion estimation technique for compression of HDTV signals," in *IEE 4th International Conference on Image Processing and Its Applications (IPA '92)*, pp. 417–420, Maastricht, The Netherlands, April 1992.

[17] F. Rovati, D. Pau, E. Piccinelli, L. Pezzoni, and J. M. Bard, "An innovative, high quality and search window independent motion estimation algorithm and architecture for MPEG-2 encoding," *IEEE Transactions on Consumer Electronics*, vol. 46, no. 3, pp. 697–705, 2000.

[18] S. Mietens, P. H. N. de With, and C. Hentschel, "Computational complexity scalable motion estimation for mobile MPEG encoding," *IEEE Transactions on Consumer Electronics*, 2002/2003.

Stephan Mietens was born in Frankfurt (Main), Germany in 1972. He graduated in Computer Science from the Technical University of Darmstadt, Germany, in 1998 on the topic of "asynchronous VLSI design." Subsequently, he joined the University of Mannheim, where he started his research on "flexible video coding and architectures" in cooperation with Philips Research Laboratories in Eindhoven, The Netherlands. He joined the Eindhoven University of Technology in Eindhoven, The Netherlands, in 2000, where he is working towards a Ph.D. degree on "scalable video systems." Since 2003, he became a Scientific Researcher at Philips Research Labs. in the Storage and System Applications group, where he is involved in projects to develop new coding techniques.

Peter H. N. de With obtained his M.S. engineering degree from the University of Technology in Eindhoven in 1984 and his Ph.D. degree from the University of Technology Delft, The Netherlands in 1992. From 1984 to 1993, he joined the Magnetic Recording Systems Department, Philips Research Labs. in Eindhoven, and was involved in several European projects on SDTV and HDTV recording. He also contributed as a principal coding expert to the DV digital camcording standard. In 1994, he joined the TV Systems group, where he was leading advanced programmable architectures design as Senior TV Systems Architect. In 1997, he became a Full Professor at the University of Mannheim, Germany, in the Faculty of Computer Engineering. In 2000, he joined CMG Eindhoven as a principal consultant and he became a Professor in Electrical Engineering Faculty, University of Technology Eindhoven (EE Faculty). He has written numerous papers on video coding, architectures, and their realization. He is a Regular Teacher of postacademic courses at external locations. In 1995 and 2000, he coauthored papers that received the IEEE CES Transactions Paper Award. In 1996, he obtained a company Invention Award. Mr. de With is an IEEE Senior Member, Program Member of the IEEE CES (Tutorial Chair, Program Chair) and Chairman of the Benelux Information Theory Community.

Christian Hentschel received his Dr.-Ing. (Ph.D.) in 1989 and Dr.-Ing. habil. in 1996 from Braunschweig University of Technology, Germany. He worked on digital video signal processing with focus on quality improvement. In 1995, he joined Philips Research Labs. in Briarcliff Manor, USA, where he headed a research project on moiré analysis and suppression for CRT-based displays. In 1997, he moved to Philips Research Labs. in Eindhoven, The Netherlands, leading a cluster for programmable video architectures. He got the position of a Principal Scientist and coordinated a project on scalable media processing with dynamic resource control between different research laboratories. Since August 2003, he is a Full Professor at the University of Technology in Cottbus, Germany, where he heads the Department of Media Technology. He is a member of the Technical Committee of the International Conference on Consumer Electronics (IEEE) and a member of the FKTG in Germany.